Ionic conductances driving tonic firing in Purkinje neurons of larval zebrafish

Meha P. Jadhav and Vatsala Thirumalai
National Centre for Biological Sciences, Tata Institute of Fundamental Research, Bellary Road, Bangalore 560065.

Keywords: calcium current, calcium-dependent potassium current, HCN current, action potential, purkinje neuron, voltage clamp.

Keypoints:

- Tonic firing is an intrinsic property of Purkinje neurons in mammals and fish.
- These neurons express multiple types of voltage-gated conductances including HCN-current, L-type and T-type calcium currents and SK- and BK-type calcium-dependent potassium currents.
- Blocking L-type calcium channels and SK-type calcium dependent potassium channels resulted in spike broadening and reduced tonic firing.
- L-type calcium currents were activated during the repolarisation of the spike.
- Based on this we conclude that calcium entry via L-type channels activates SK- channels causing faster repolarization of the spike and therefore sustained tonic firing.

Abstract:

Purkinje neurons are the principal neuronal types in the cerebellum, which is among the oldest and most conserved regions of the vertebrate brain. In mammals and in larval zebrafish, Purkinje neurons can generate tonic firing even when isolated from the network. Here we investigated the ionic basis of tonic firing in the Purkinje neurons of larval zebrafish using voltage clamp

isolation of membrane currents along with pharmacology. We discovered that these neurons express hyperpolarization and cyclic nucleotide gated (HCN) inward currents, L-type high voltage activated calcium currents, T-type low-voltage activated calcium currents and SK and BK type calcium activated potassium currents. Among these, L-type calcium currents and SK-type calcium-dependent potassium currents were indispensable for tonic firing, while blocking HCN, T-type and BK currents had little effect. We observed that action potentials were broadened when either L-type or SK channels were blocked. Based on these results, we propose that calcium entry via L-type calcium channels activates SK potassium channels leading to faster action potential repolarization, in turn aiding the removal of inactivation of sodium channels. This allows larval zebrafish Purkinje neurons to continue to fire tonically for sustained periods. In mammals also tonic firing in Purkinje neurons is driven by calcium channels coupling to calcium-dependent potassium channels, yet the specific types of channels involved are different. We therefore suggest that coupling of calcium channels and calcium-dependent potassium channels could be a conserved mechanism for sustaining long bouts of high frequency firing.

Author contributions: MPJ: Conceptualization, investigation, analysis and writing; VT: Conceptualization, analysis, and writing.

Competing interests: Authors declare that they have no competing interests.

Data and materials availability: All data are available in the main text or the supplementary materials. Before final acceptance, we will upload data and analysis scripts available on Zenodo.

Acknowledgments
The authors would like to thank the funding agencies listed below and Mr. P.T. Jagadeesh for the maintenance of our fish lines.

Funding:

Wellcome Trust-DBT India Alliance Intermediate fellowship 500040/Z/09/Z (VT)

Wellcome Trust-DBT India Alliance Senior fellowship IA/S/17/2/503297 (VT)

Department of Biotechnology BT/PR4983/MED/30/790/2012 (VT)

Science and Engineering Research Board EMR/2015/000595 (VT)

Department of Atomic Energy (VT)

NCBS-TIFR graduate student fellowship (MPJ)

Introduction

The cerebellum is one of the most highly conserved regions of the vertebrate brain: the cell types, gene expression patterns and connectivity are highly homologous among all vertebrate classes from fish to mammals (Nieuwenhuys, 1967; Bell, 2002; Bae et al., 2009). This is particularly true for Purkinje neurons (PNs), which are the principal neurons of the cerebellar cortex and have similar molecular markers, dendritic morphology and connectivity across all vertebrates (Bae et al., 2009; Robra and Thirumalai, 2016; Kidd, 2017). PNs are critical for cerebellar function and their impairment leads to loss of motor co-ordination (Taroni and DiDonato, 2004; Chopra and Shakkottai, 2014). While the electrical properties of PNs have been well studied in mammals (Llinás and Sugimori, 1980; Raman and Bean, 1999; Womack and Khodakhah, 2003; Häusser et al., 2004), less is known in other vertebrates. Investigating the ionic basis of PN activity in non-mammalian vertebrates is important for understanding key properties essential for its functioning.

In zebrafish, PNs are specified by 3 days post fertilization (dpf) (Bae et al., 2009; Hamling et al., 2015) and stable electrical activity patterns can be observed as early as 5 dpf (Sengupta and Thirumalai, 2015). In addition, calcium imaging and ablation studies report that the PN population participates in natural behaviors of larval zebrafish at these stages (Ahrens et al., 2012; Markov et al., 2021). Given the relative ease of cell identification, single cell recording and pharmacology in larval zebrafish, we chose to investigate the ionic basis of PN activity in this model system.

In vivo recordings show that like mammalian PNs, larval zebrafish PNs (zPNs) exhibit simple spikes mediated by TTX-sensitive sodium channels and that they can fire spontaneously even when isolated from the network (Sengupta and Thirumalai, 2015). Like mammalian PNs, these neurons also elaborate dendritic arbors in the molecular layer and receive synaptic inputs from parallel fibers of granule cells and climbing fibers (CF) of the inferior olive (Bae et al., 2009; Sitaraman et al., 2021).

While the cerebellar circuitry and PN physiology are largely conserved across vertebrates (Fig. 1A), there are some differences between the firing properties of PNs in rodents versus zebrafish. Simple spikes are attenuated in the soma and complex spikes are completely absent, unlike mammalian PNs. Also, zPNs exhibit bistability, while this is a subject of debate for mammalian PNs (Loewenstein et al., 2005; Schonewille et al., 2006; Engbers et al., 2013; Sengupta and Thirumalai, 2015). These differences suggest underlying differences in the biophysics of PNs across these two systems. However, the kinds of ionic conductances expressed in zebrafish PNs and their contribution to spontaneous activity is largely unknown.

Our earlier work showed that zPNs can exist in one of two stable membrane potential states: when in the depolarized state, they fire tonically and when hyperpolarized, they fire in bursts. Tonic firing is an intrinsic property of zPNs that persists even in the absence of synaptic inputs (Sengupta and Thirumalai, 2015), similar to mammalian PNs. Here, we investigate the ionic conductances responsible for tonic firing in zPNs. We show that these cells have a large calcium current contributed by L and T-type calcium channels with little to no contribution from P/Q type channels. Blocking L-type calcium channels or SK-type calcium dependent potassium channels had the same effect: a decrease or a complete cessation of tonic firing. Blocking SK channels also leads to a shallower AHP which reduces the pool of available sodium channels to drive tonic activity. Together, our results show that L-type and SK channels are critical for maintaining high-frequency tonic firing in zPNs.

Results

Spontaneous activity in Purkinje Neurons

We performed whole-cell patch clamp electrophysiology from PNs *in vivo* in larval zebrafish at 5-8 days post fertilization (dpf) (Fig. 1B). As has been reported previously, zPNs display two distinct firing modes: tonic and bursting (Fig. 1C, D). We were also able to switch the state of the cell by supplying a

constant current. Both the modes show the presence of both sodium-mediated simple spikes as well as climbing fiber (CF) EPSPs. The two modes also differ in several key characteristics: membrane potential, firing frequencies of simple spikes, and their dependence on synaptic input. We plotted the distribution of membrane potential at each data point from the traces in Fig. 1C and D, after applying a median filter to isolate the low frequency membrane potential changes. While the distribution for the tonic state is unimodal, that for the bursting state is bimodal (Fig. 1E). The modes of these distributions, referred to as basal membrane potential, are also different (Fig. 1F). The inter-spike intervals (ISI) of simple spikes are more variable for the tonic and bursting mode (Fig. 1G). This difference in inter-spike interval can also be seen as difference in the bursting index. Bursting index was quantified as mean of ISI divided by the median of ISI. Consequently, if the neuron is firing at regular intervals, the bursting index will be closer to 1. A higher bursting index indicates more variability in ISI and therefore more bursts (Fig. 1H).

Sengupta and Thirumalai, 2015 have shown that the cells can maintain tonic firing even in the absence of synaptic inputs. On the other hand, CF inputs can trigger bursts when zPNs are in the hyperpolarized state and calcium spikes when they are depolarized above spike threshold (Fig. 1I, arrow). Further, zPNs displayed sag potentials when hyperpolarized (Fig. 1J, arrow). These results suggest that zPNs have significant high threshold calcium currents and hyperpolarization-activated inward currents. It is also obvious that the tonic firing mode is dependent on intrinsic properties of zPNs unlike the bursting mode which is activated by synaptic inputs.

Therefore, we wished to determine the major ion channels involved in maintaining tonic firing in these neurons. To do this, we measured cellular currents in voltage clamp mode and also compared spontaneous activity of zPNs when specific channel types were blocked with antagonists. We quantified several parameters including basal membrane potential, simple spike amplitudes, rates, shapes, etc., and compared them across the two conditions.

I_h does not contribute to tonic firing

We first performed voltage clamp to measure the hyperpolarization activated inward current I_h in zPNs. We provided second-long voltage pulses from -100 mV to -20 mV (Fig. 2A). Measurements were done in the presence of TTX (1 μM) and TEA (1 mM) to block sodium and potassium currents respectively. Since cesium blocks I_h, these recordings were performed with recording solutions containing potassium gluconate. We used ZD7288, a selective blocker of hyperpolarization and cyclic nucleotide gated (HCN) channels that mediate the I_h current. All recordings are paired, i.e currents were measured in the same cell before and after addition of HCN channel blocker ZD7288. A slowly activating inward current, between -100 and -70 mV (Fig. 2B) that was sensitive to 50 μM ZD7288 could be observed in all zPNs (n=8) that we recorded from (Fig. 2A, B).

We then examined the effect of I_h block on the spontaneous activity of zPNs (Fig. 2C-D). We observed that blocking I_h had no significant effect on the neuron's spontaneous activity. The cells were able to fire both tonically and in bursts. The firing rate of simple spikes in the tonic mode and the bursting index remained unchanged (Fig. 2C-F). We also did not observe a significant difference in the distribution of membrane potentials across the two modes as compared to control (Fig. 2G). We therefore concluded that I_h plays no significant role in the regulation of bistability or in the maintenance of tonic firing in zPNs.

Voltage-gated calcium channels regulate tonic firing

We next wanted to understand how calcium currents shape the spontaneous activity of zPNs *in vivo*. For this, we first performed voltage clamp experiments to measure the total calcium currents. As shown in Fig. 3A, we delivered voltage command pulses in the presence of TTX and TEA and measured cellular currents before and after application of 10 μM cadmium chloride, a nonspecific, high voltage-gated calcium channel blocker. A cadmium-sensitive inward current with peak values at a holding potential of -20mV was observed in all cells we recorded from (Fig. 3A-C).

Next, we recorded from zPNs in current clamp mode under bursting and tonic-firing conditions before and after application of 10 μM cadmium chloride. We recorded the state of the cell without current injection and then made it switch states by injecting depolarizing or hyperpolarizing current. After perfusing the antagonist in the bath, we recorded from the same cell again in both states (Fig. 3D).

We found that the cells could still fire in both states even in the presence of cadmium (Fig. 3E, H). 4 out of 11 cells switched states upon the addition of cadmium while the rest continued to fire in the same state. Although basal membrane potential in both states did not change, tonic firing of simple spikes was affected. Simple spikes became less frequent and were smaller in amplitude (Fig. 3F, G). ISIs became more irregular, with a higher coefficient of variance (CV of ISI in tonic mode for control: 0.81 ± 0.06; cadmium: 1.73 ± 0.11). 3 of the 11 cells went into depolarization-induced block later in the recording. We did not observe any drastic changes in the bursting behavior and the bursting index remained the same in cadmium compared to control (Fig. 3I, J).

The above results show that suggest a role for voltage-gated calcium channels in tonic firing. Application of cadmium in the bath affects voltage-gated channels everywhere, including those that mediate neurotransmission. To rule out network-mediated effects and to test this in a cell specific manner, we next blocked calcium channels intracellularly using the calcium chelator 1,2-bis(o-amino phenoxy) ethane-N,N,N′,N′- tetraacetic acid (BAPTA). We recorded from cells using normal patch internal solution or with 20 mM of BAPTA. Cells recorded with BAPTA internal were also able to fire in both states (Fig. 3K, N), however simple spike rate decreased, while spike amplitude remained the same (Fig. 3L, M). Bursting index and the spike rate within bursts remained unaffected (Fig. 3O, P), underlining the importance of calcium currents in regulating tonic firing specifically.

Calcium currents in zPNs are primarily driven by L and T-type channels

Neurons express many different types of voltage-gated calcium channels, with distinct kinetics and effects on neuronal firing properties. We wanted to determine the classes of voltage-gated calcium channels expressed in zPNs. Takeuchi et al., 2016 analyzed the transcriptome of 12 dpf zPNs. From their dataset, we looked for the expression levels of genes encoding voltage-gated calcium channels and found significant expression of transcripts encoding L-type, P/Q type and T-type channel subunits, with L-type showing highest levels of expression (Fig. 4A). Auxiliary subunits of calcium channels were also strongly expressed.

Supported by this dataset, we set out to measure calcium currents in zPNs using voltage clamp protocols and pharmacology. We recorded the current response of cells to a series of voltage pulses in the presence of 1 μM TTX and 1mM TEA. We recorded the response in normal saline and after application of different calcium channel antagonists and plotted their current-voltage (I-V) relationships. As before, we observed a large inward current active between -50 mV and +20 mV (Fig. 4B-E) which was partially blocked by the T-type channel blocker, Mibefradil. In 100 μM Mibefradil, the peak inward current was reduced to 50% of the control values. Addition of 100 μM of the L-type channel blocker Nifedipine further decreased the peak inward current to 10% of the control values (Fig. 4B, C). On the other hand, application of the P/Q type channel blocker, ω-agatoxin IVA (100 nM) reduced the current by only 9 percent (Fig 4.E, H). We also found that blocking P/Q channels had no significant effect on the tonic firing rate in Purkinje cells (Mean firing rate control: 7.78 $\pm$ 1.75 Hz; ω-agatoxin IVA: 6.90 Hz $\pm$ 1.68; data not shown).

Overall, we find that the L and T-type calcium channels are major contributors to voltage-gated calcium current. It also suggests that the P/Q- type channels contribute minimally, if at all. It is also possible that ω-agatoxin IVA is not an effective blocker of P/Q- type channels in zebrafish.

We next asked how each of these channel types contributed to the tonic firing in these cells.

L-type, but not T-type channels are required for sustained tonic firing

To understand the contribution of T-type calcium channels to tonic firing in zPNs, we recorded their firing behavior before and after application of the T-type channel blocker, Mibefradil. Unlike cadmium and intracellular BAPTA, application of 40 μM Mibefradil failed to alter tonic firing frequency or amplitude (Fig. 5A-C). These data show, that T-type channels are not significant contributors to tonic firing in zPNs.

Next, we recorded from zPNs in current clamp mode before and after application of the L-type channel blocker, Nifedipine. The effects were similar to that of adding cadmium. In the tonic mode, simple spikes had slightly reduced frequency but the amplitude was not significantly different (Fig. 5D-F). Nifedipine also changed the shape of the spike (Fig. 5G), as evidenced by an increase in spike width and decay time (Fig. 5I, J).

L-type calcium currents are active during spike repolarization

Calcium imaging studies from PNs show calcium entry and elevation of cytosolic calcium levels during simple spike firing (Ramirez and Stell, 2016), suggesting that voltage-gated calcium channels are activated during simple spike firing. To confirm if L-type channels are indeed active during simple spike firing in zPNs and to explore their possible role in repolarization, we replayed a train of simple spikes as a voltage command. We found that replaying the simple spike waveform as recorded at the soma (eg., Fig. 1C) did not recruit sodium channels. This could be because the spike initiation zone for these neurons is in the axon initial segment and the waveform was too weak to activate sodium channels in this region. Scaling up the amplitude of simple spikes led to a significant sodium current (data not shown). We, therefore, decided to use a scaled-up version of the simple spike waveform (~2.5x of original).

To quantify the calcium currents, all experiments were done in the presence of sodium and potassium channel antagonists (TTX and TEA). We found a significantly large, inward current in response to the simple spike waveform. We also saw that this current was slow to activate and achieved maximum amplitude well beyond the peak of a simple spike, corresponding to the repolarization and AHP phases of the simple spike (Fig. 6H). Importantly, this current was sensitive to Nifedipine (Fig. 6H, K).

These experiments show that L-type channels are indeed active when the cell fires simple spikes. The channels achieve peak activation after the peak of the simple spike, during the repolarization phase.

BK channels also contribute to membrane repolarization but do not modulate tonic firing frequency

We were surprised to find that the L-type calcium channels were active during the repolarization phase and that blocking them increased spike width. Both these observations could be explained if these effects were mediated by calcium-dependent potassium channels (KCa). If this were true, the effect of blocking KCa channels should mimic the effect of blocking L-type calcium channels. Typically, KCa channels can be of large (BK), intermediate (IK) or small (SK) conductance. Of these BK and SK channels are known to be important for spike repolarization and AHP.

We first tested whether BK channels couple with L-type channels and contribute to membrane repolarization. However, blocking BK channels with 100 nM Iberiotoxin, had no effect on the tonic firing frequency of these channels (Fig. 6A-C). However, similar to L-type block, we observed a slight broadening of the simple spike but no changes in the AHP amplitude (Fig. 6D-G).

We also examined whether zPNs could generate simple spikes in a sustained manner upon depolarization, before and after application of Iberiotoxin (Fig. 6H). There was no change in the spike adaptation ratio

(Frequency of first spike/ Frequency of 10th spike) or spiking threshold (Fig. 6I-L). This suggests that while BK channels may contribute to membrane repolarization, they do not control the firing frequency of simple spikes.

SK channels couple to L-type channels to sustain tonic firing

We observed that blocking small conductance (SK) channels with apamin did indeed mimic the effects of L-type channel block (Fig. 7A). Simple spikes were smaller and less frequent in the tonic mode (Fig. 7B, C). They also became broader and the AHP shallower pointing toward their role in the repolarization of simple spikes (Fig. 7D-G).

These data show that L-type calcium channels maintain the tonic firing of simple spikes and contribute to spike repolarization by activating SK channels.

SK currents sustain high-frequency firing for a long duration by increasing sodium channel availability

The input resistance and rheobase of the cells did not change significantly in the presence of either apamin or nifedipine, showing that the excitability of cells remained the same (data not shown). To test if SK channels contribute to sustained firing, we depolarized zPNs and recorded their firing responses. We added synaptic blockers (NBQX and gabazine) in the bath and provided a negative current to hyperpolarize the cell to -70 mV. In this way, the cells were silent unless depolarized. In response to a two-second-long pulse, the cells did not show any spike adaptation across the entire pulse under control conditions,. On the other hand, in the presence of apamin, the cells fired simple spikes for up to 500 ms and then became irregular or silent (Fig. 7H). On average, the cells fired fewer spikes in apamin and had a higher spike adaptation ratio (Fig. 7K).

Lower repolarization and shallower AHP can reduce sodium channel recovery from inactivation. With time, this can reduce the availability of these

channels and prevent the cell from generating more spikes. This usually leads to a depolarized threshold and a decrease in the maximum dv/dt of a spike (Colbert et al., 1997; Vandael et al., 2012). We did indeed observe this with apamin (Fig. 7I, J, L, M).

Overall, these data show that L-type calcium channels and SK calcium-dependent potassium channels are important for sustaining tonic firing for longer durations. They do so by allowing membrane repolarization and maintaining sodium channel availability.

Discussion

The larval zebrafish provides an excellent system where neuronal physiology can be studied *in vivo*, in an intact circuit. Our study sheds some light on how ionic mechanisms drive tonic firing in an *in vivo* preparation. Here, we have shown that zPNs express interesting membrane potential dynamics driven by diverse channel types. We identified hyperpolarization activated inward current I_h, high- and low- voltage-gated calcium currents and calcium activated potassium currents in these neurons. Together with SK-type KCa channels, L-type calcium channels contribute to the repolarization of membrane potential and AHP of simple spikes. They allow cells to fire tonically for a long duration in the up state by increasing the availability of sodium channels. BK channels also contribute to repolarization but not to the simple spike frequency and AHP. Overall, we show that L-type voltage-gated calcium channels and SK calcium-activated potassium channels are important in maintaining tonic firing in the up state of zPNs (Fig. 8). Further work can help shed light on the ionic mechanisms of bistability in Purkinje cells.

Limitations of the study

Pharmacological studies are most limited by a lack of specificity. We applied all antagonists in the external milieu of the fish, blocking a class of channels throughout the brain. Because of this, when comparing firing patterns,

we cannot completely negate the effect of altered synaptic inputs. Nevertheless, our BAPTA experiments show that the effects of a calcium channel block on simple spike firing rate are mainly due to intrinsic changes. Still, we cannot rule out any off-target effects of the channel antagonists or that they have reduced affinity for their intended targets in zebrafish. To address the latter, we performed voltage clamp experiments to test if the blockers affected cellular currents in their expected voltage range. For example, the I_h blocker ZD7288 reduced cellular currents in the hyperpolarized voltage range (Fig. 2B) and the L-type channel blocker Nifedipine blocked cellular currents in the depolarized voltage ranges (Fig. 4B), as expected. These results attest to the specificity of these agents towards their intended target. The negative results with agatoxin and iberiotoxin could also be due to their limited interactions with zebrafish P/Q-type and BK channels respectively and therefore, these negative results should be interpreted cautiously.

In this study, we focused on channels that affected the tonic state. None of these channels seemed to affect spiking in the bursting state. Bursting requires synaptic input and when GABAergic and glutamatergic inputs are blocked, zPNs become quiescent upon hyperpolarization. A full investigation of mechanisms driving bursting and those governing switches from one state to another is necessary to fully understand PN dynamics. One challenge is the high variability of bursting within and among cells. A higher sample size (both in the duration of recordings and the number of cells) might allow us to find subtle changes in bursting parameters.

Our study captures the bistability and contribution of calcium currents in a small developmental window. All of the experiments were done on larvae between the ages of 5-8 dpf. By this stage, the major components of the cerebellar circuitry are in place and Purkinje cells display their characteristic firing. However, this is still an early developmental stage and the circuit undergoes further maturation. The cerebellum grows in volume with a concurrent increase in Purkinje cell numbers (Bae et al., 2009; Hamling et al., 2015). During this time, PNs elaborate dendritic arbors in the molecular layer

and make numerous synaptic contacts with parallel and climbing fibers (Sitaraman et al., 2021). But, not much is known about maturation of ion channel distributions in zPNs. In rodents, it is well appreciated that the first two weeks of post-natal life is a period of drastic developmental changes in the cerebellum (van Welie et al., 2011) with changes in firing properties (McKay and Turner, 2005), ion channel distributions (Womack and Khodakhah, 2003; Hosy et al., 2011), and synaptic pruning (Hashimoto and Kano, 2013). It is likely that zPNs also undergo such developmental transformation during early larval stages and these processes remain to be studied.

Physiology of Purkinje neurons in teleosts and mammals

Purkinje cells in teleosts share many of the properties of mammalian PNs as has been shown in this and in many previous studies. PNs in teleosts and in mammals are arranged in a monolayer and send elaborate dendritic arbors into the molecular layer where they receive numerous excitatory and inhibitory synaptic inputs from conserved cell types and pathways (Meek, 1992). Studies localizing protein markers have been carried out extensively in rodent PNs and in zebrafish PNs. Both rodent PNs and zPNs express the dopamine and cAMP regulated phospho protein Darpp32 also known as ppp1r1b (Ouimet et al., 1984, 1992; Robra and Thirumalai, 2016). Expression of Glutamate receptor delta 2 is also seen in both cases (Araki et al., 1993; Mikami et al., 2004; Tam et al., 2021). In contrast, Zebrin II expression shows distinct expression patterns in rodent and zebrafish PNs: in rodents, PNs are organized into alternating Zebrin II -positive and negative stripes whereas in zebrafish, the expression is uniform in all PNs (Brochu et al., 1990; Bae et al., 2009).

Both mammalian PNs and teleost PNs receive excitatory inputs from parallel fibers and climbing fibers and fire simple spikes spontaneously (Sengupta and Thirumalai, 2015; Pose-Méndez et al., 2023). In rodents, PNs seem to exhibit bistable behavior, with an ‘up’ state where they fire action potentials and a ‘down’ state where they are quiescent and may fire bursts (Williams et al., 2002; Womack and Khodakhah, 2002). Excitatory climbing fiber inputs or inhibitory input from molecular layer interneurons could toggle PNs

between these states (Loewenstein et al., 2005; Oldfield et al., 2010; Engbers et al., 2013). Nevertheless, bistability in rodents PNs *in vivo* is contested due to the effect of anesthetics on PN physiology (Schonewille et al., 2006) . We have shown previously that zPNs are bistable and that stimulating climbing fibers triggers bursts (Sengupta and Thirumalai, 2015). While I_h seems to shape PN bistability in rodents (Williams et al., 2002), it seems to not play a major role in zPNs. However, the specificity of ZD7288 for zebrafish HCN channels is not established and even in rodents, ZD7288 has off-target effects (Wu et al., 2012). Further experiments are needed to assess this finding more closely such as with zebrafish mutants lacking HCN channel subunits.

Calcium and calcium-activated potassium currents in PNs

Much of what we know regarding ionic conductances underlying PN activity comes from experiments performed in rodent cerebellar slices acutely, or PNs in dissociated culture. These studies have shown that calcium currents activated by the action potential are mainly carried by P/Q-type and T-type voltage-gated calcium channels (Raman and Bean, 1999; Swensen and Bean, 2003). Calcium entry through these channels activates BK and SK calcium-dependent potassium channels and for this reason, blocking calcium channels or KCa potassium channels produces the same effect on spontaneous firing of PNs (Womack and Khodakhah, 2002, 2003; Edgerton and Reinhart, 2003). Our experiments on zPNs point to some similarities and differences. Like in mammals, fish PNs also regulate spontaneous tonic firing via calcium channels and calcium-dependent potassium channels. But, in zPNs, calcium enters via the L-type and not the P/Q type calcium channels. While P/Q type channels are coupled to SK channels in rodents, we find that L-type channels are coupled to SK channels in fish. Neuronal firing is regulated by the coupling of calcium channels and calcium-dependent channels in many other neuronal types as well such as in hippocampal pyramidal neurons (Lancaster et al., 1991), midbrain dopaminergic neurons (Wolfart and Roeper, 2002), neurons in the medial vestibular nucleus (Smith et al., 2002) etc. In each case, the voltage-gated calcium channel through which calcium enters and the type of calcium-

dependent potassium channels it is coupled to are different. Together with our results, these studies suggest that coupling of calcium and calcium-dependent potassium channels is a conserved mechanism for regulating neuronal firing properties across vertebrates and across neuronal types.

Methods

Fish rearing and care:

The use of all experimental animals (*Danio rerio*) was approved by the Institutional Animal Ethics Committee (IAEC) and the Institutional Biosafety Committee (IBSC). Wild type zebrafish were used for all experiments. All adults were housed in a continuous recirculating system (Tecniplast, Italy). Conductivity and pH of water were maintained at 1200mS and 7.2 respectively. The adults were bred to obtain embryos. Once collected, embryos were maintained in small tanks without constant circulation. Methylene blue (0.0005%) was added to the water from the recirculation system and this was used to raise the larvae until the day of the experiments. Adults were fed Zeigler diet and brine shrimp nauplii while larvae were fed Zeigler Larval Diet. Both adults and larvae were maintained at 28^{o} C with a 14:10 hour light:dark cycle. All experiments were performed on larvae at 5-8 dpf.

Whole-cell patch clamp

Animal preparation

Larvae were anesthetized with 0.01% MS222 and then transferred onto a block of Sylgard (Dow Corning, Midland, MI, United States) in the middle of the recording chamber. Tungsten wire (California Fine Wire, Grover Beach, CA, United States) was used to pin the tail, head and jaws to the Sylgard block. Next, the MS222 was replaced with external saline (composition in mM; 134 sodium chloride, 2.9 potassium chloride, 1.2 magnesium chloride, 10 HEPES, 10 Glucose, 2.1 calcium chloride, 0.01 alpha tubocurarine; pH:

7.8; 290 mOsm). Using a pair of fine forceps, the skin covering the brain was gently peeled off.

Electrodes and cell identification

Pipettes were pulled from thick walled borosilicate capillaries (1.5 mm OD; 0.86 mm ID; Harvard Apparatus, Massachusetts, United States) using a Flaming Brown P-97 pipette puller (Sutter Instruments, Novato, CA, United States) such that they had a tip diameter of ~1 μm and resistances in the range of 12-17 MΩ when filled with internal solution. Large, elliptical cells in the dorsal region of the cerebellum were targeted for whole-cell patch clamp. They were confirmed as Purkinje cells based on the large CF-EPSCs and their characteristic firing profile in the current clamp (Sengupta and Thirumalai, 2015). The recording solution also contained sulphorhodamine (30µg/mL) and the fill of the cell was also observed to confirm the characteristic morphology of Purkinje cells.

Recording solutions

For current clamp recordings, pipettes were filled with potassium gluconate-based internal solution (composition in mM: 115 potassium gluconate, 15 potassium chloride, 2 magnesium chloride, 10 HEPES, 10 EGTA, 4 Mg-ATP; pH: 7.2; 290 mOsm). In experiments where 20 mM tetra K-BAPTA (Life Technologies) was added, concentration of potassium gluconate was reduced to 35 mM with the rest of the components unchanged.

For voltage clamp recordings, cesium gluconate internal solution was used (composition in mM: 115 cesium hydroxide, 115 gluconic acid, 15 cesium chloride, 2 sodium chloride,10 HEPES, 10 EGTA, 4 Mg-ATP; pH 7.2; 290 mOsm).

Data acquisition

Whole-cell recordings were acquired using Multiclamp 700B amplifier, Digidata 1440A digitizer and pCLAMP software (Molecular Devices). The data was low pass filtered at 2 kHz using a Bessel filter and sampled at 50 kHz at a gain of 10. The capacitive currents were compensated using the amplifier circuitry. In case of voltage clamp recordings, leak currents were subtracted. The recordings are not corrected for liquid-liquid junction potential which has earlier been estimated to be +8mV for the K gluconate based internal solution (Sengupta and Thirumalai, 2015). Neurons with resting membrane potential above -30 mV and with series resistance higher than 10% input resistance were excluded. Series resistance was measured at regular intervals during the recordings. Cells in which it had changed by more than 25% in the course of the experiment were excluded.

Pharmacology

All pharmacological agents except BAPTA were superfused in the bath. Recordings from the same cell prior to antagonist superfusion were considered as control. Recordings were made after the 5-6 minutes of perfusion of the pharmacological agent. The complete list of the chemicals used and their concentrations is given in table 1.

Chemical name	**Make**	**Catalog number**	**Concentration used**
Apamin	Hello Bio	HB1051	200 nM
Cadmium chloride	Sigma Aldrich	202908	10 µM
Gabazine (SR-95531)	Sigma Aldrich	S106	10 µM
Iberiotoxin	Hello Bio	HB1053	100 nM
K4-BAPTA	Life Technologies	B1024	20 mM
Mibefedril	Sigma Aldrich	M5441	100 µM
NBQX	Tocris	373	20 µM

Nickel chloride	Sigma Aldrich	223387	30 μM
Nifedipine	Sigma Aldrich	N7634	200 μM
ω-Agatoxin IVA	Hello Bio	HB1212	100 nM
TEA Bromide	Sigma Aldrich	241059	1 mM
Tetrodotoxin	Hello Bio	HB1035	1mM
ZD7288	Sigma Aldrich	Z3777	20 μM

Table 1: List of pharmacological agents used for this study.

Analysis

All traces were analyzed and plotted using ClampFit 10.7 and custom scripts written in MATLAB (MathWorks Inc). To estimate baseline membrane potential, the traces were first passed through a median filter to remove fast membrane potential changes due to spikes. For the tonic state, basal membrane potential was taken as the mode of membrane potential distribution of the filtered trace. In case of the bursting state, the membrane potential had a bimodal distribution and the two modes were considered as the two baseline membrane potentials. An amplitude threshold was used to distinguish the climbing fiber inputs from the simple spikes. Bursts were defined as any group of three or more spikes with interval less than 300ms. The decay time is time required to settle back to 10% of peak amplitude. Action potential width was calculated at half amplitude. Threshold was determined to be 4 percent of maximal dv/dt value. AHP values were calculated as the difference between threshold and the most hyperpolarized point immediately following the peak of the actional potential.

Statistics

Figure 1					
Parameter	**Tonic**	**Bursting**	**Statistical test**	**p value**	
Basal membrane potential (mV)	-46.6373	-60.5	Mann-Whiteny U test	9.04E-08	
CV of inter spike interval	0.9448	1.2615		0.0167	
Bursting Index	1.44	1.94		0.0114	
Figure 2					
Parameter	**Control**	**ZD7288**	**Statistical test**	**p value**	
Maximum inward current at -100 mV	145.7870	50.4411	Wilcoxon signed rank	0.0078	
Maximum inward current at -90 mV	108.4476	41.2340		0.0078	
Maximum inward current at -80 mV	78.3682	24.2657		0.0078	
Simple spike rate (Hz)	9.85	7.21		0.5513	
Bursting index	2.7268	2.5915		0.8457	
Intraburst simple spike rate (Hz)	6.5386	6.2765		0.6875	
Basal membrane potential for tonic (mV)	-48.8333	-49.5		0.8125	
Basal membrane potential for burst (mV)	-62.6667	-63.1667		0.6875	
Figure 3					
Parameter	**Control**	**Cadmium**	**Statistical test**	**p value**	
Peak inward current at -20 mV	302.933	128.175	Wilcoxon signed rank	4.88e-4	
Amplitude of simple spikes (mV)	20.62	13.15		0.00097600	
Simple spike rate (mV)	10.49	5.96		0.00195313	
Bursting index	1.9928	1.5366		0.0840	
Intraburst simple spike rate (mV)	7.6657	8.1332		0.365234375	
Parameter	**Control**	**BAPTA**	**Statistical test**	**p value**	

Amplitude of simple spikes (mV)	20.62	15.83	Mann-Whiteny U test	0.09	
Simple spike rate (mV)	9.43	5.88		0.0018141	
Bursting index	1.9928	1.9366		0.876	
Intraburst simple spike rate (mV)	5.1811	6.0009		0.1618	
Figure 4					
Parameter	**Control**	**Antagonist1**	**Antagonist2 (mib+nif)**	**Statistical test**	**p value**
Maximum inward current (pA) (mibefradil +nifedipine)	361.9175	175.51	33.4336	Friedman's Test	0.000747
Maximum inward current (pA) (agatoxin)	366.0251	290.7441			0.0178
Figure 5					
Parameter	**Control**	**Mibefradil**	**Statistical test**	**p value**	
Amplitude of simple spikes (mV)	18.88	16.45	Wilcoxon signed rank	0.0537	
Simple spike rate (Hz)	7.3505	7.4094		0.9658	
Parameter	**Control**	**Nifedipine**	**Statistical test**	**p value**	
Ampltiude of simple spikes (mV)	16.85	14.72	Wilcoxon signed rank	0.31	
Simple spike rate (Hz)	6.99	3.47		0.01	
Decay time (ms)	3.3921	4.3801		0.021	
Spike width (ms)	2.6575	3.3750		0.034	
Peak inward current (pA)	493.2421	170.129		9.77E-04	
Figure 6					
Parameter	**Control**	**Iberiotoxin**	**Statistical test**	**p value**	
Ampltiude of simple spikes (mV)	22.21	19.53	Wilcoxon signed rank	0.3	
Simple spike rate (Hz)	10.12	8.92		0.22	
Decay time (ms)	7	12.8		0.02	
Spike width (ms)	5.13	9.4		0.02	
Ampltiude of AHP (mV)	10.17	7.32		0.08	
Spike threshold (mV)	-47.55	-45.82		0.06	
Spike adaptation ratio	1.3978	1.0983		0.5781	
Figure 7					

Parameter	Control	Apamin	Statistical test	p value	
Ampltiude of simple spikes (mV)	18.07	13.81	Wilcoxon signed rank	0.13	
Simple spike rate (Hz)	9.78	5.13		0.0039	
Decay time (ms)	7.67	11.92		0.03	
Spike width (ms)	5.62	10.66		0.01	
Amplitude of AHP (mV)	15.82	10.45		0.0039	
Spike threshold (mV)	-46.7941	-43.7201		0.03	
Spike adaptation ratio	1.03	2.71		0.0045	
Maximum dv/dt (V/s)	7.4714	3.1814		0.002	

Reference:

Ahrens MB, Li JM, Orger MB, Robson DN, Schier AF, Engert F, Portugues R (2012) Brain-wide neuronal dynamics during motor adaptation in zebrafish. Nature 485:471–477.

Araki K, Meguro H, Kushiya E, Takayama C, Inoue Y, Mishina M (1993) Selective Expression of the Glutamate Receptor Channel δ2 Subunit in Cerebellar Purkinje Cells. Biochemical and Biophysical Research Communications 197:1267–1276.

Bae Y-K, Kani S, Shimizu T, Tanabe K, Nojima H, Kimura Y, Higashijima S, Hibi M (2009) Anatomy of zebrafish cerebellum and screen for mutations affecting its development. Dev Biol 330:406–426.

Bell CC (2002) Evolution of cerebellum-like structures. Brain Behav Evol 59:312–326.

Brochu G, Maler L, Hawkes R (1990) Zebrin II: A polypeptide antigen expressed selectively by purkinje cells reveals compartments in rat and fish cerebellum. Journal of Comparative Neurology 291:538–552.

Chopra R, Shakkottai VG (2014) Translating cerebellar Purkinje neuron physiology to progress in dominantly inherited ataxia. Future Neurol 9:187–196.

Colbert CM, Magee JC, Hoffman DA, Johnston D (1997) Slow Recovery from Inactivation of Na+ Channels Underlies the Activity-Dependent Attenuation of Dendritic Action Potentials in Hippocampal CA1 Pyramidal Neurons. J Neurosci 17:6512–6521.

Edgerton JR, Reinhart PH (2003) Distinct contributions of small and large conductance Ca2+-activated K+ channels to rat Purkinje neuron function. J Physiol 548:53–69.

Engbers JDT, Fernandez FR, Turner RW (2013) Bistability in Purkinje neurons: Ups and downs in cerebellar research. Neural Networks 47:18–31.

Hamling KR, Tobias ZJC, Weissman TA (2015) Mapping the development of cerebellar Purkinje cells in zebrafish. Dev Neurobiol 75:1174–1188.

Hashimoto K, Kano M (2013) Synapse elimination in the developing cerebellum. Cell Mol Life Sci 70:4667–4680.

Häusser M, Raman IM, Otis T, Smith SL, Nelson A, Lac S du, Loewenstein Y, Mahon S, Pennartz C, Cohen I, Yarom Y (2004) The Beat Goes On: Spontaneous Firing in Mammalian Neuronal Microcircuits. J Neurosci 24:9215–9219.

Hosy E, Piochon C, Teuling E, Rinaldo L, Hansel C (2011) SK2 channel expression and function in cerebellar Purkinje cells. The Journal of Physiology 589:3433–3440.

Kidd K (2017) A Comparative Analysis of Purkinje Cells Across Species Combining Modelling, Machine Learning and Information Theory. Available at: http://uhra.herts.ac.uk/handle/2299/21078 [Accessed October 6, 2023].

Lancaster B, Nicoll RA, Perkel DJ (1991) Calcium activates two types of potassium channels in rat hippocampal neurons in culture. J Neurosci 11:23–30.

Llinás R, Sugimori M (1980) Electrophysiological properties of in vitro Purkinje cell dendrites in mammalian cerebellar slices. J Physiol 305:197–213.

Loewenstein Y, Mahon S, Chadderton P, Kitamura K, Sompolinsky H, Yarom Y, Häusser M (2005) Bistability of cerebellar Purkinje cells modulated by sensory stimulation. Nat Neurosci 8:202–211.

Markov DA, Petrucco L, Kist AM, Portugues R (2021) A cerebellar internal model calibrates a feedback controller involved in sensorimotor control. Nat Commun 12:6694.

McKay BE, Turner RW (2005) Physiological and morphological development of the rat cerebellar Purkinje cell. The Journal of Physiology 567:829–850.

Meek J (1992) Comparative aspects of cerebellar organization. From mormyrids to mammals. Eur J Morphol 30:37–51.

Mikami Y, Yoshida T, Matsuda N, Mishina M (2004) Expression of zebrafish glutamate receptor δ2 in neurons with cerebellum-like wiring. Biochemical and Biophysical Research Communications 322:168–176.

Nieuwenhuys R (1967) Comparative Anatomy of the Cerebellum. In: Progress in Brain Research (Fox CA, Snider RS, eds), pp 1–93 The Cerebellum. Elsevier. Available at: http://www.sciencedirect.com/science/article/pii/S0079612308609620 [Accessed November 14, 2018].

Oldfield CS, Marty A, Stell BM (2010) Interneurons of the cerebellar cortex toggle Purkinje cells between up and down states. Proc Natl Acad Sci U S A 107:13153–13158.

Ouimet CC, Lamantia AS, Goldman-Rakic P, Rakic P, Greengard P (1992) Immunocytochemical localization of DARPP-32, a dopamine and cyclic- AMP-regulated phosphoprotein, in the primate brain. Journal of Comparative Neurology 323:209–218.

Ouimet CC, Miller PE, Hemmings HC, Walaas SI, Greengard P (1984) DARPP-32, a dopamine- and adenosine 3’:5’-monophosphate-regulated phosphoprotein enriched in dopamine-innervated brain regions. III. Immunocytochemical localization. J Neurosci 4:111–124.

Pose-Méndez S, Schramm P, Valishetti K, Köster RW (2023) Development, circuitry, and function of the zebrafish cerebellum. Cell Mol Life Sci 80:227.

Raman IM, Bean BP (1999) Ionic currents underlying spontaneous action potentials in isolated cerebellar Purkinje neurons. J Neurosci 19:1663–1674.

Ramirez JE, Stell BM (2016) Calcium Imaging Reveals Coordinated Simple Spike Pauses in Populations of Cerebellar Purkinje Cells. Cell Reports 17:3125–3132.

Robra L, Thirumalai V (2016) The Intracellular Signaling Molecule Darpp-32 Is a Marker for Principal Neurons in the Cerebellum and Cerebellum-Like Circuits of Zebrafish. Front Neuroanat 10:81.

Schonewille M, Khosrovani S, Winkelman BHJ, Hoebeek FE, De Jeu MTG, Larsen IM, Van der Burg J, Schmolesky MT, Frens MA, De Zeeuw CI (2006) Purkinje cells in awake behaving animals operate at the upstate membrane potential. Nat Neurosci 9:459–461; author reply 461.

Sengupta M, Thirumalai V (2015) AMPA receptor mediated synaptic excitation drives state-dependent bursting in Purkinje neurons of zebrafish larvae. Elife 4.

Sitaraman S, Yadav G, Agarwal V, Jabeen S, Verma S, Jadhav M, Thirumalai V (2021) Gjd2b-mediated gap junctions promote glutamatergic synapse formation and dendritic elaboration in Purkinje neurons Cline HT, Stainier DY, Cline HT, Watt AJ, eds. eLife 10:e68124.

Smith MR, Nelson AB, du Lac S (2002) Regulation of Firing Response Gain by Calcium-Dependent Mechanisms in Vestibular Nucleus Neurons. Journal of Neurophysiology 87:2031–2042.

Swensen AM, Bean BP (2003) Ionic Mechanisms of Burst Firing in Dissociated Purkinje Neurons. J Neurosci 23:9650–9663.

Tam WY, Wang X, Cheng ASK, Cheung K-K (2021) In Search of Molecular Markers for Cerebellar Neurons. Int J Mol Sci 22:1850.

Taroni F, DiDonato S (2004) Pathways to motor incoordination: the inherited ataxias. Nat Rev Neurosci 5:641–655.

van Welie I, Smith IT, Watt AJ (2011) The metamorphosis of the developing cerebellar microcircuit. Curr Opin Neurobiol 21:245–253.

Vandael DHF, Zuccotti A, Striessnig J, Carbone E (2012) CaV1.3-Driven SK Channel Activation Regulates Pacemaking and Spike Frequency Adaptation in Mouse Chromaffin Cells. J Neurosci 32:16345–16359.

Williams SR, Christensen SR, Stuart GJ, Häusser M (2002) Membrane potential bistability is controlled by the hyperpolarization-activated current I(H) in rat cerebellar Purkinje neurons in vitro. J Physiol (Lond) 539:469–483.

Wolfart J, Roeper J (2002) Selective Coupling of T-Type Calcium Channels to SK Potassium Channels Prevents Intrinsic Bursting in Dopaminergic Midbrain Neurons. J Neurosci 22:3404–3413.

Womack M, Khodakhah K (2002) Active Contribution of Dendrites to the Tonic and Trimodal Patterns of Activity in Cerebellar Purkinje Neurons. J Neurosci 22:10603–10612.

Womack MD, Khodakhah K (2003) Somatic and Dendritic Small-Conductance Calcium-Activated Potassium Channels Regulate the Output of Cerebellar Purkinje Neurons. J Neurosci 23:2600–2607.

Wu X, Liao L, Liu X, Luo F, Yang T, Li C (2012) Is ZD7288 a selective blocker of hyperpolarization-activated cyclic nucleotide-gated channel currents? Channels (Austin) 6:438–442.

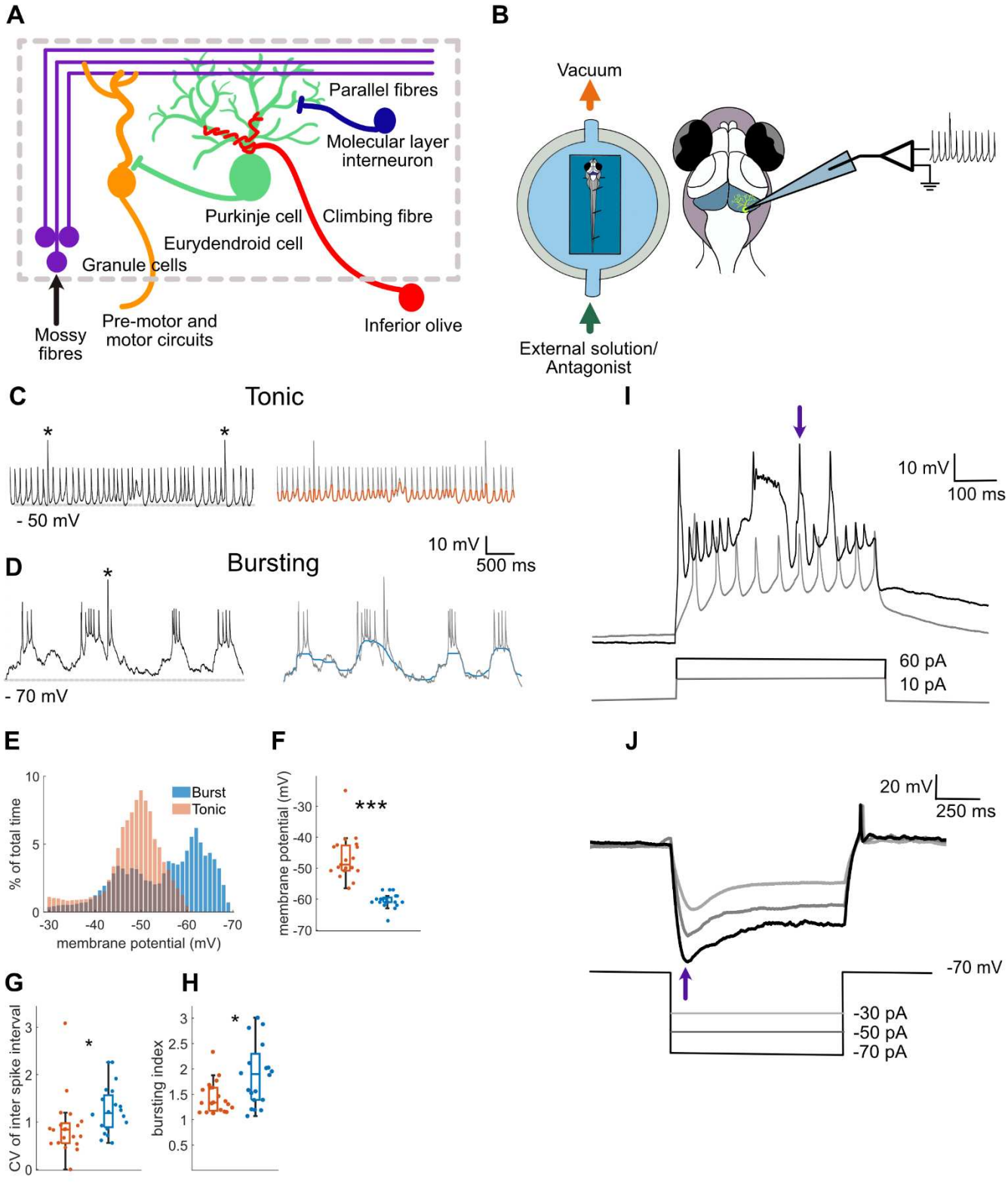

Figure 1 Spontaneous activity in Purkinje cells. **A.** Schematic showing the preparation for in vivo whole-cell recording of Purkinje neurons (PN). **B.** Location of the cerebellum in the larval zebrafish brain, highlighted in blue. The cerebellar circuitry showing the major inputs to the PNs and their postsynaptic targets. **C.** Representative trace of a tonic firing cell (top). * Indicates climbing fibre driven EPSPs. The same trace after application of median filter (blue) to show membrane potential changes on a longer time scale (bottom). **D.** Same as E for a bursting cell. **D. E.** Distribution of membrane potentials of the traces in C and D after applying median filter. Tonic cell in blue and bursting in orange. **F.** Basal membrane potentials of cells in tonic and burst mode. For burst, the lower basal membrane potential was used. **G.** Coefficient of variance of simple spike intervals in tonic and bursting cells. **H.** Bursting index for tonic and bursting cells (mean ISI/ mode ISI) N=20 in each mode**;** *$p<0.05$, ***$p<0.001$, Mann-Whitney U Test. **I.** Response of Purkinje cells to depolarising current pulses. Lower input current generates sodium driven simple spikes (gray trace) while a higher input current elicits large amplitude and broader calcium spikes (black trace). Arrow indicates a calcium spike. **J.** Response of Purkinje cells to hyperpolarising current pulses. Note the sag (arrow) in the early part of the pulse and rebound spike after the pulse. This indicates presence of HCN current in the cell.

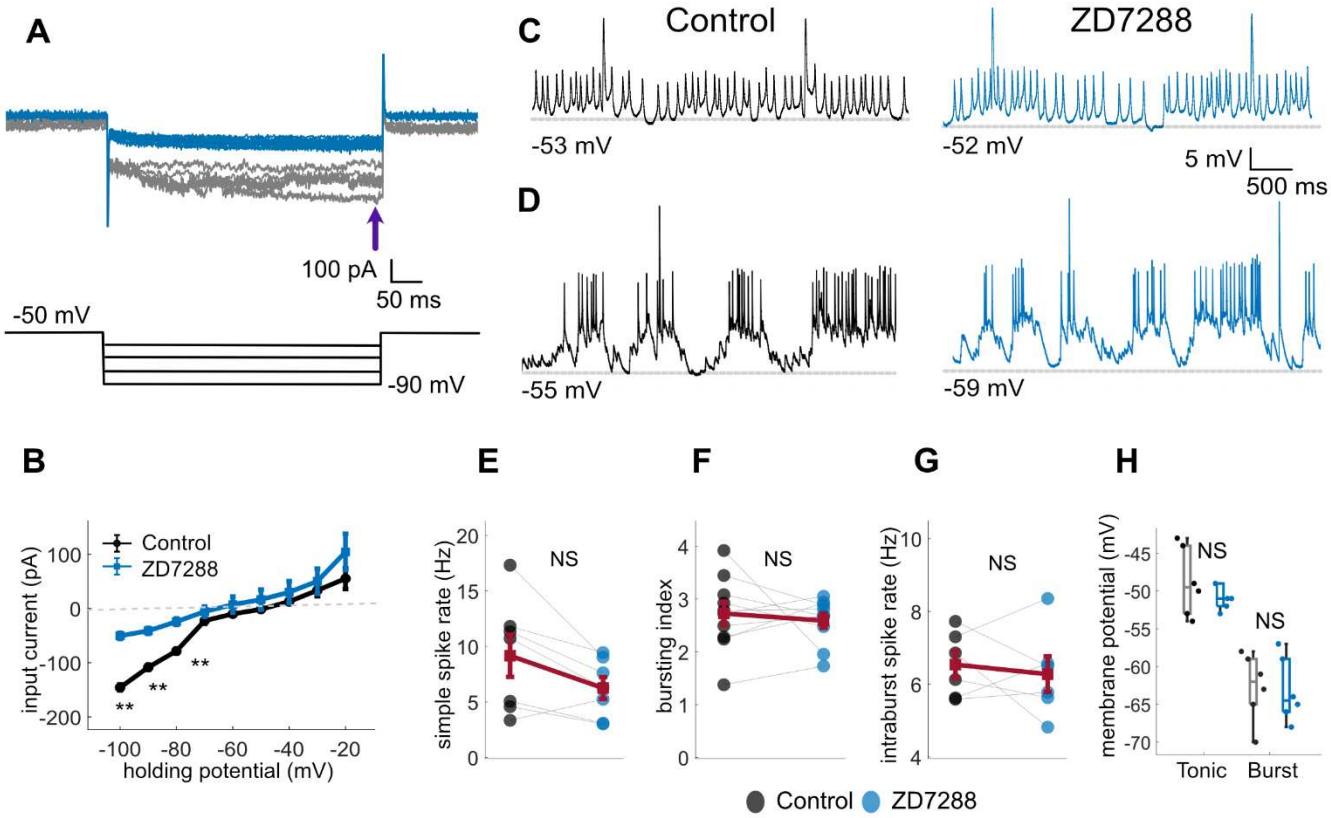

Figure 2 Blocking HCN channels has no significant effect on Purkinje cell activity. **A.** Voltage command used to activate HCN and the corresponding current response in a representative trace. Mean current measured from highlighted region. **B.** Steady state current in before and after addition of ZD7288. HCN current can be seen as an inward current between -100 to -70 mV (N=8). **C-D.** Representative traces of cells firing in tonic and bursting mode before and after addition of HCN antagonist ZD7288. **E-H.** Simple spike tonic firing rate, bursting index of burst cells, intra-burst simple spike rate and membrane potential of tonic and bursting cells before and after addition of ZD7288. N=6; **p<0.01 Wilcoxon signed rank test.

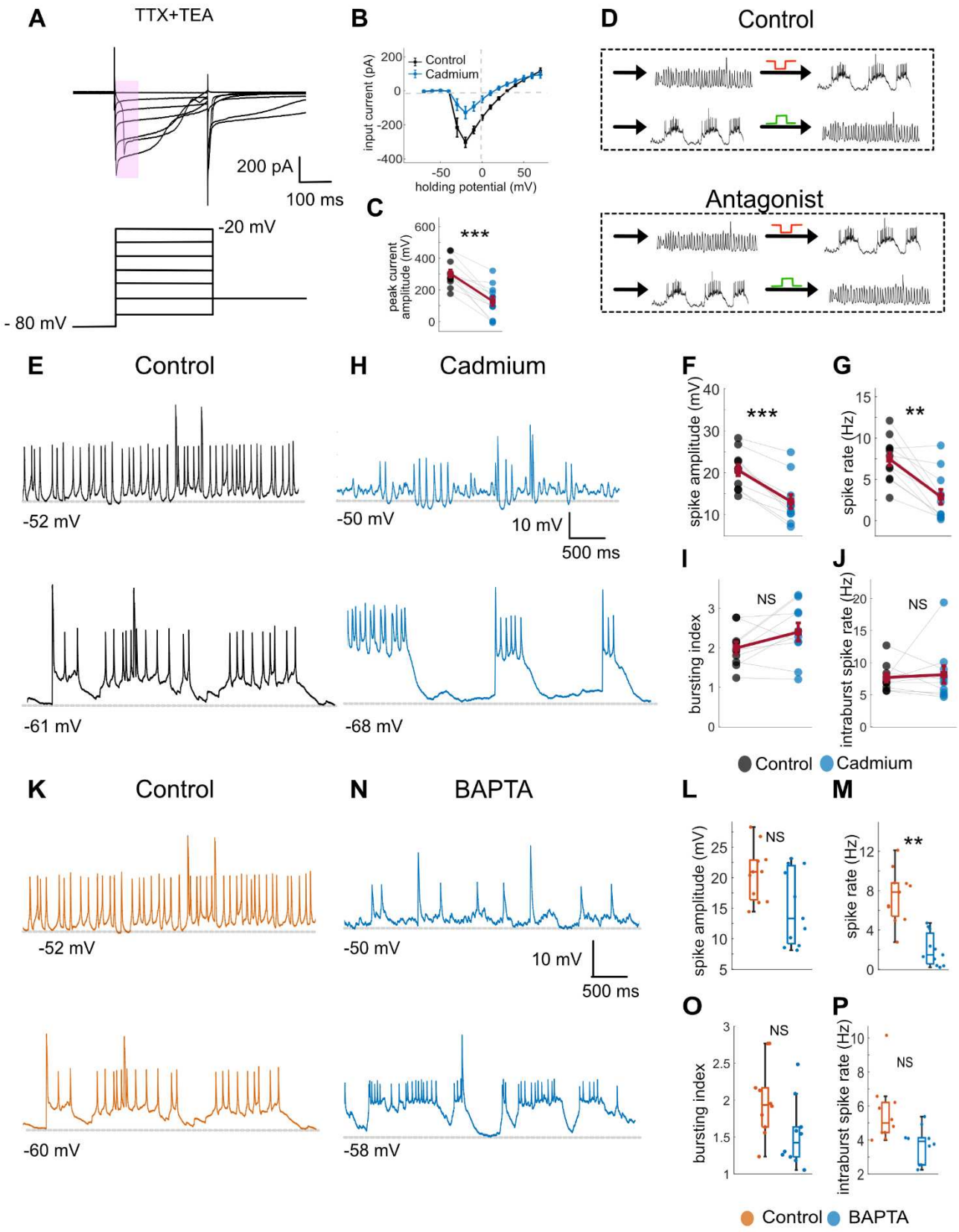

Figure 3 Blocking calcium channel affects tonic firing of simple spikes independent of synaptic inputs. **D.** Protocol used for paired spontaneous recordings of PN. Each cell was recorded from in both tonic and bursting state before (control) and after addition of the channel antagonist. **A.** Schematic representing the command voltage given and a corresponding representative current response of cell in the presence of TTX (1µM) and TEA bromide (1mM). **E and H.** Representative traces of tonic and bursting cells before (black) and after addition of cadmium chloride (10µM) (blue). **B.** Average IV response of cells before and after addition of cadmium chloride. **C.** The maximum inward current at -20 mV in cells before and after cadmium chloride. **F-G.** Mean simple spike rate and amplitude in tonic firing cells without and with cadmium. **I-J.** Bursting index and intra-burst simple spike rate before and after cadmium chloride. N=11; **p<0.01, ***p<0.001, NS=p>0.05 Wilcoxon signed rank test. **K and N.** Representative traces of cells firing tonically and in bursts with BAPTA in the recording pipette. **L-M.** Mean simple spike rate and amplitude in tonic firing cells in control cells versus BAPTA. **O-P.** Bursting index intra-burst simple spike rate in control and BAPTA. N=11; Mann-Whitney U Test; ***p<0.001, NS=p>0.05.

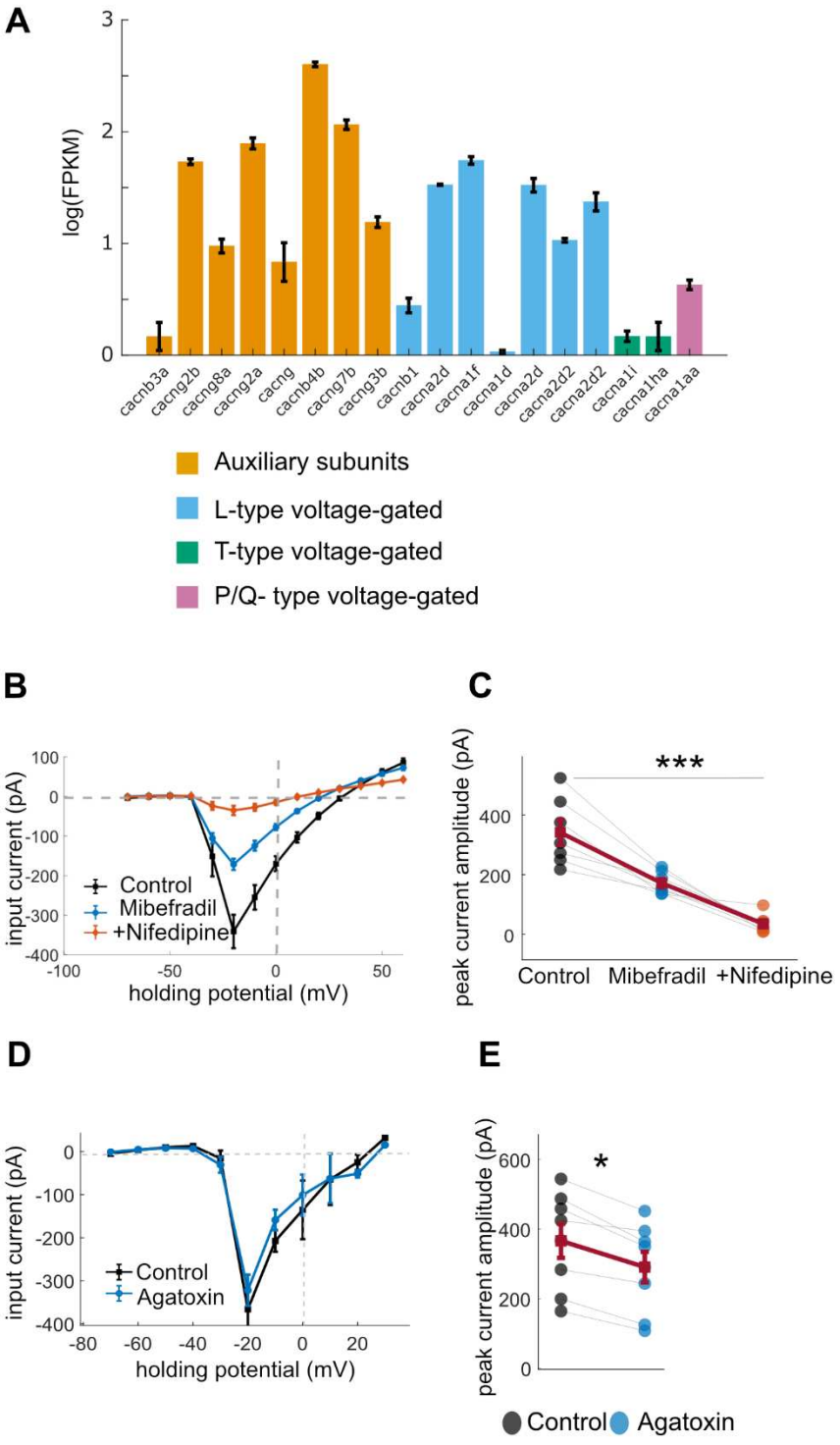

Figure 4 Calcium current in Purkinje cells is mainly contributed by L and T type voltage gated calcium channels. **A.** mRNA levels of genes for voltage-gated calcium channels in 12dpf larval zebrafish. (Data from Takeuchi et. Al., 2016). Average IV response of cells **B.** Without antagonist (black), with T-type channel antagonist mibefradil (orange) (40 µM) followed by L-type channel antagonist, nifedipine (blue) (100µM). **D.** before and after addition of ω-agatoxin IVA (100 nM). The maximum inward current at -20 mV in cells **C.** in control, with mibefradil and nifedipine. N=10; Friedman's test; ***$p<0.001$. **E.** before and after addition of ω-agatoxin IVA. N=8; Wilcoxon signed-rank test; *$p<0.05$.

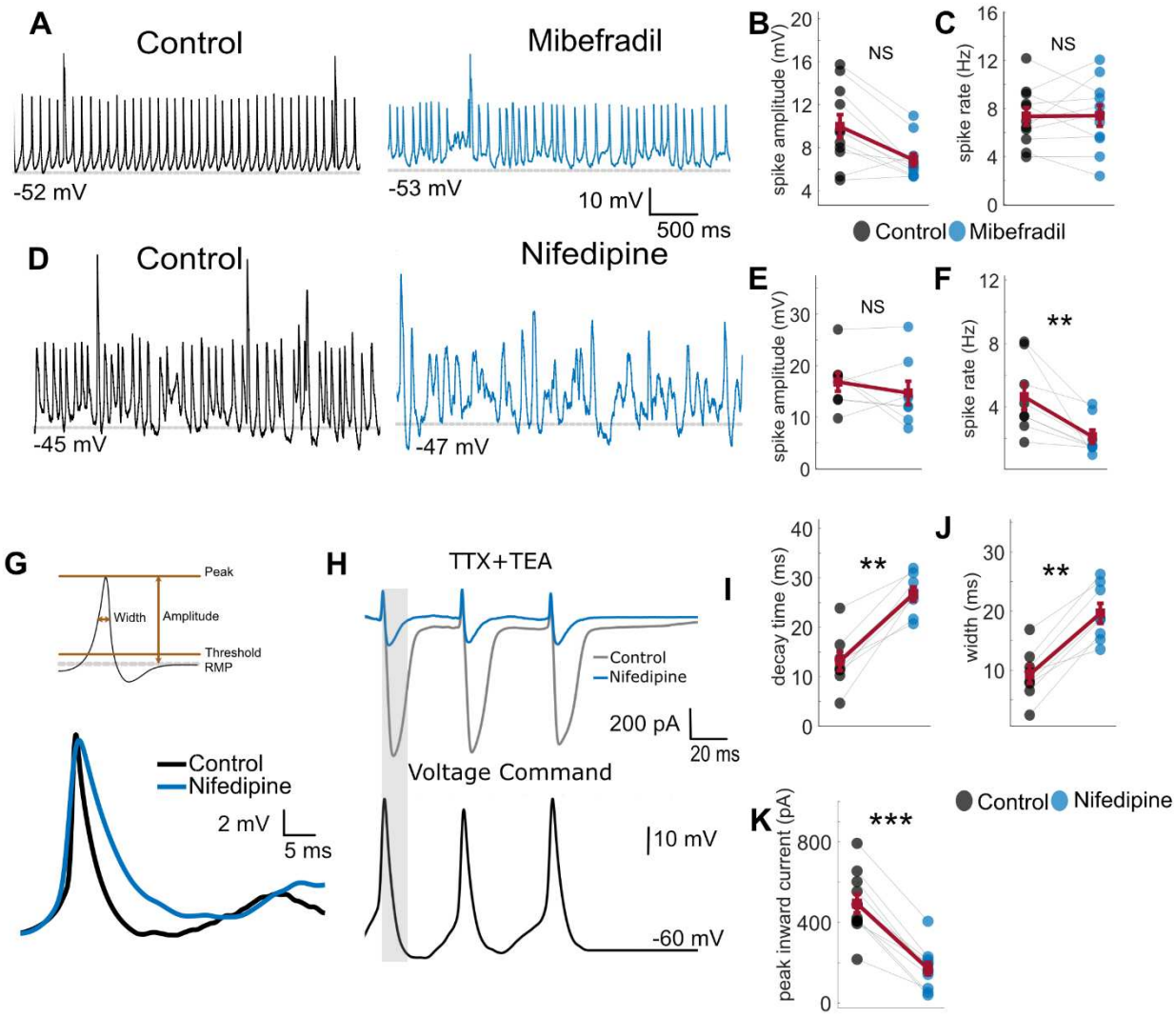

Figure 5 L-type and not T-type channel are important for tonic firing and membrane repolarisation. **A.** Representative traces of tonic firing before and after addition of T-type antagonist, mibefradil (40µM). **B-C.** Mean simple spike amplitude and spike rate in control and in presence of mibefradil. (N=11). **D.** Representative traces of tonic firing before and after addition of L-type antagonist, nifedipine (100µM). **E-F.** Mean simple spike amplitude and spike rate in control and in presence of nifedipine (N=8). **G.** Averaged simple spike waveform from one representative cell before (black) and after addition of nifedipine (blue). **H.** Simple spike waveform given as voltage command and a representative current response of cell without and with nifedipine. Experiments were performed in the presence of TTX (1µM) and TEA (1mM). **I-J.** Decay time and width of simple spikes during tonic firing

before and after addition of nifedipine (N=8). **K.** Peak inward current in response to simple waveform as a voltage command without and with nifedipine (N=10). Wilcoxon signed-rank test; **p<0.01, ***p<0.001, NS p>0.05.

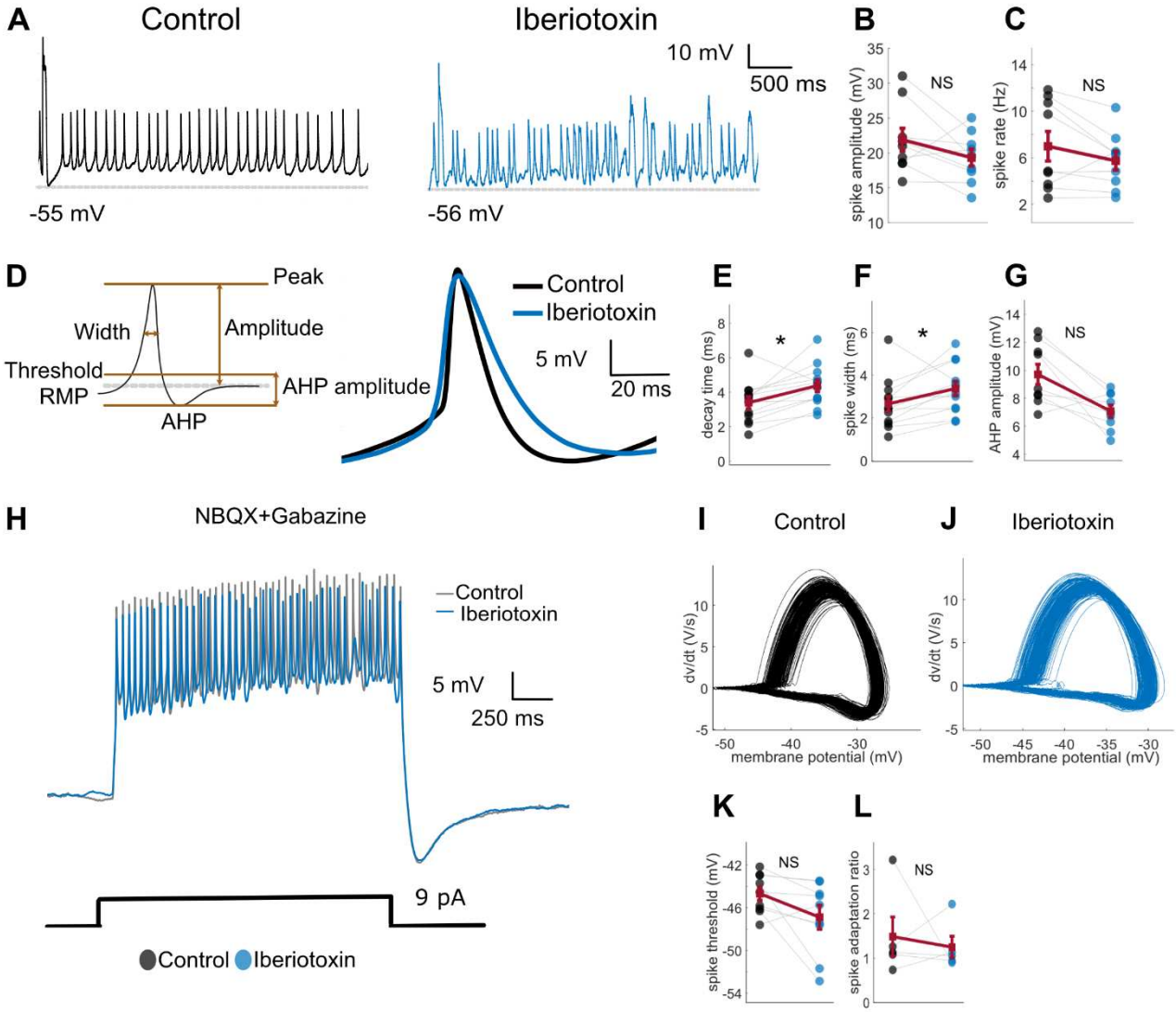

Figure 6 BK channels also contribute to membrane repolarisation but do not modulate tonic firing frequency. **A.** Representative trace of a tonic firing cell before and after addition of BK channel antagonist, iberiotoxin (100 nM). **B-C.** Mean simple spike amplitude and frequency before and after addition of apamin (N=9). **D.** Averaged simple spike waveform from one representative cell before (black) and after addition of apamin (blue). **E-G.** Mean decay time, width and AHP amplitude of simple spikes (N=10). **H.** Representative response of a cell to a depolarising pulse of current before and after addition of iberiotoxin. These experiments were done in the presence of synaptic blockers NBQX (20µM) and Gabazine (10 µM). A constant negative current was applied to keep the cell membrane potential at ~-70 mV. **I-J.** Phase plane of all simple spikes in a representative cell in control and with iberiotoxin. **K-L.** Mean

spike adaptation ratio and spiking threshold in control condition and with iberiotoxin (N=10). Wilcoxon signed-rank test; *p<0.05, **p<0.01, ***p<0.001, NS=p>0.05.

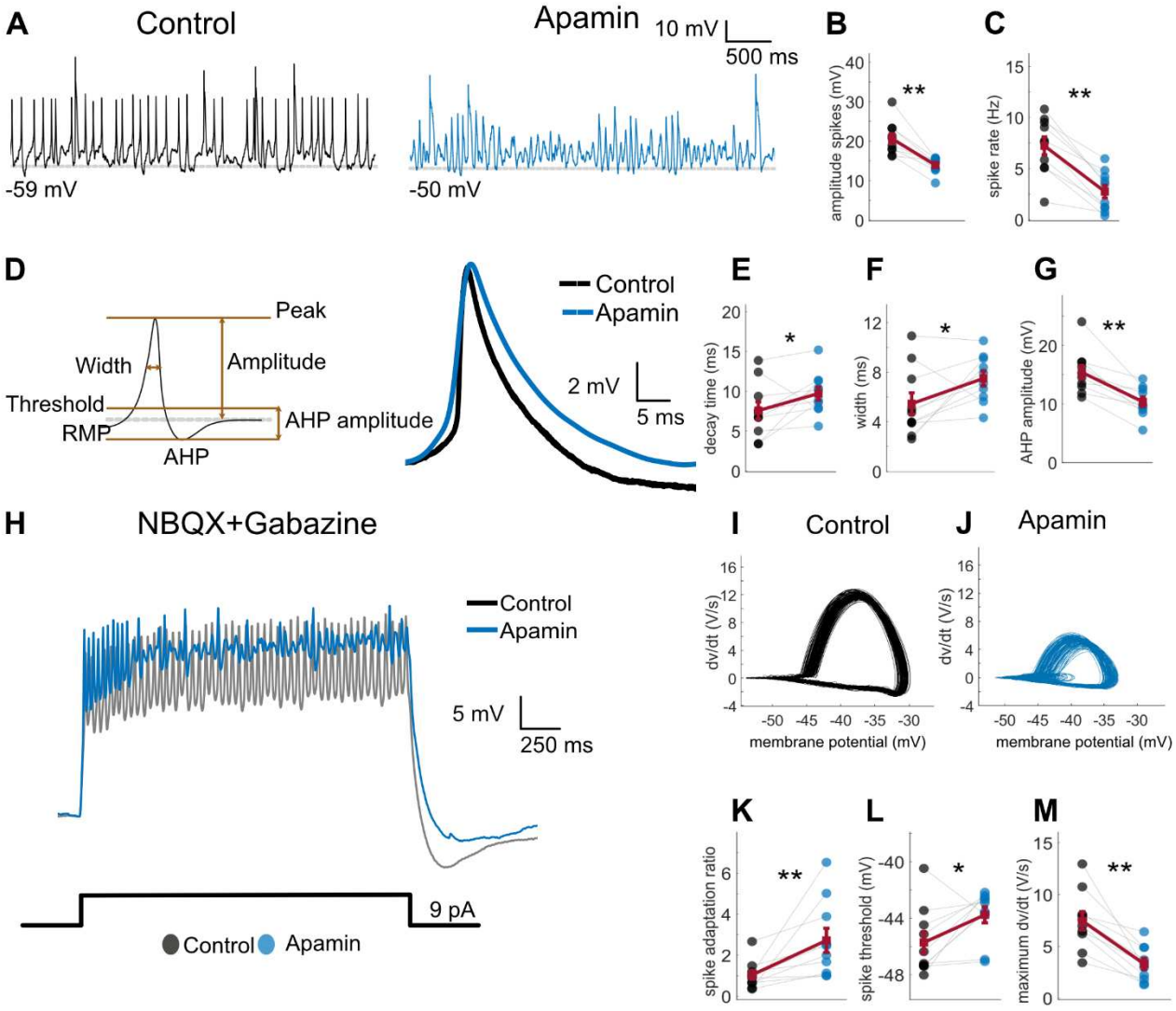

Figure 7 SK channels allow cells to maintain tonic firing by regulating sodium channel availability. **A.** Representative trace of a tonic firing cell before and after addition of SK channel antagonist, apamin (200 nM). **B-C.** Mean simple spike amplitude and frequency before and after addition of apamin (N=10). **D.** Averaged simple spike waveform from one representative cell before (black) and after addition of apamin (blue). **E-G.** Mean decay time, width and AHP amplitude of simple spikes (N=10). **H.** Representative response of a cell to a depolarising pulse of current before and after addition of apamin. These experiments were done in the presence of synaptic blockers NBQX (20µM) and Gabazine (10 µM). **I-J.** Phase plane of all simple spikes in a representative cell in control and with apamin. **K-M.** Mean

spike adaptation ratio, spiking threshold and maximum dv/dt of simple spikes in response to current pulse in control condition and with apamin (N=10). Wilcoxon signed-rank test; *p<0.05, **p<0.01, ***p<0.001.

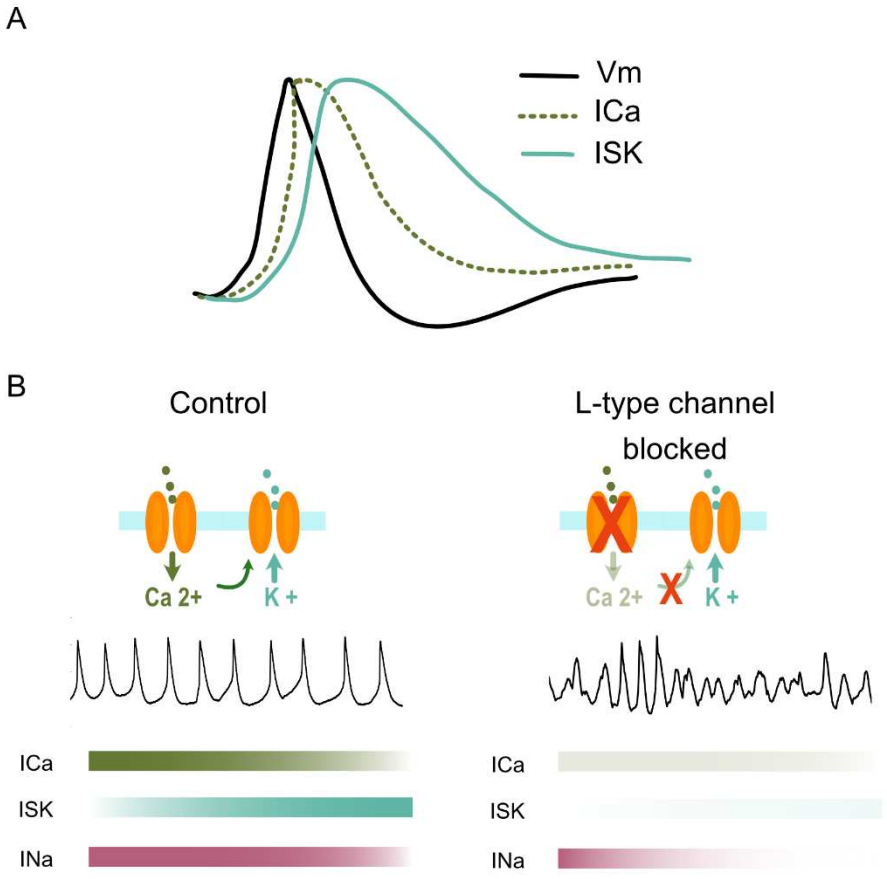

Figure 8 L-type channels couple with calcium activated potassium SK channels to maintain tonic firing in zPNs. A: Time course of activation of L-type calcium currents (dotted line) and SK-potassium currents (green line) during an action potential (black). B: Schematic showing coupling of L-type calcium channels to SK-potassium channels in control and L-type channel block conditions. The colored bars indicate slow build-up of the corresponding currents during tonic firing.